

Virtual Knot Cobordism and the Affine Index Polynomial

Louis Hirsch Kauffman
 Department of Mathematics, Statistics
 and Computer Science (m/c 249)
 851 South Morgan Street
 University of Illinois at Chicago
 Chicago, Illinois 60607-7045
 <kauffman@uic.edu>

Abstract

This paper studies cobordism for virtual knots. Non-trivial examples of virtual slice knots are given and determinations of the four-ball genus of positive virtual knots are explained in relation to joint work with Dye and Kaestner. We study the affine index polynomial, prove that it is a concordance invariant for knots and links (explaining when it is defined for links), show that it is invariant also under certain forms of labeled cobordism and study a number of examples in relation to these phenomena.

AMS Subject classification: 57M25

Keywords: Knot, link, knotoid, virtual knot, invariant, cobordism, labeled cobordism, concordance, Khovanov homology, Rasmussen invariant, affine index polynomial.

1 Introduction

This paper defines a theory of cobordism for virtual knots and studies the cobordism invariance of the affine index polynomial [36], denoted $P_K(t)$. This invariant is also called the *writhe polynomial*, $W_K(t)$, in the context of Gauss diagrams, see [1] where the W notation is used and where a related polynomial is denoted by $P_K(t)$ (We trust there will be no confusion.). In this paper we work in the context of virtual knot and link diagrams and extend the definitions in [36] to an affine index polynomial for links (with affine labeling as described in the body of the paper). We prove that this generalized invariant is a concordance invariant of knots and links.

The paper is organized as follows. In Section 2 we review basics of virtual knot theory, the bracket polynomial and Jones polynomial for virtual knots, virtual knots with unit Jones polynomial, parity and interpretations of virtual knot theory. In Section 3 we review virtual link cobordism [16] and discuss the four-ball genus of virtual links, recalling the construction of the virtual Seifert surface for a virtual link and the theorem [3] that the four-ball genus of a positive virtual link is equal to the genus of its virtual Seifert surface. In Section 4 we re-develop the affine index polynomial [36] extending its definition to labeled links and proving that it is a concordance invariant of virtual knots and links. The reader should note that concordance invariance of the affine index polynomial for knots is proved in [1] by Gauss diagram techniques. In the present work we use affine labelings of the knot and link diagrams. In this context, we generalize the theorem to include links that are compatible with affine

labeling. We also show how the affine index polynomial is invariant under certain cobordisms of knots and links that are compositions of saddle moves at crossings that have null weights in the affine labeling. This cobordism invariance was already observed in [16] and here it is useful in understanding the core locus of the non-triviality of the polynomial. We illustrate this comment with a number of examples in the body of the paper.

Remark. *Knotoids* are knot and link diagrams with free ends in possibly distinct regions, taken up to Reidemeister moves that never move an arc across an endpoint. The subject of link cobordism and our results about the affine index polynomial in this paper all apply as well to the cobordism of knotoids. See [6, 7] for our work on knotoids. In these papers we show how to define the affine index polynomial in the category of knotoids. In particular the theorems about concordance invariance of the affine index polynomial are valid in the knotoid category. This subject of cobordism of knotoids will be taken up in a paper distinct from the present work.

We should also mention the following papers on virtual knot theory that are useful background, but not cited directly in the present paper [35, 28, 38, 13, 30, 36, 15, 27, 34, 35, 12, 31] and [25, 41, 32, 18, 19, 37, 38, 39].

2 Virtual Knot Theory

Knot theory studies the embeddings of curves in three-dimensional space. Virtual knot theory [28, 29, 30, 31] studies the embeddings of curves in thickened surfaces of arbitrary genus, up to the addition and removal of empty handles from the surface. Virtual knots have a special diagrammatic theory, described below. Classical knot theory embeds in virtual knot theory.

In the diagrammatic theory of virtual knots one adds a *virtual crossing* (see Figure 1) that is neither an over-crossing nor an under-crossing. A virtual crossing is represented by two crossing segments with a small circle placed around the crossing point.

Moves on virtual diagrams generalize the Reidemeister moves for classical knot and link diagrams. See Figure 1. Classical crossings interact with one another according to the usual Reidemeister moves, while virtual crossings are artifacts of the structure in the plane. Adding the global detour move to the Reidemeister moves completes the description of moves on virtual diagrams. In Figure 1 we illustrate a set of local moves involving virtual crossings. The global detour move is a consequence of moves (B) and (C) in Figure 1. The detour move is illustrated in Figure 2. Virtual knot and link diagrams that can be connected by a finite sequence of these moves are said to be *equivalent* or *virtually isotopic*.

Another way to understand virtual diagrams is to regard them as representatives for oriented Gauss codes [8], [28, 29] (Gauss diagrams). Such codes do not always have planar realizations. An attempt to embed such a code in the plane leads to the production of the virtual crossings. The detour move makes the particular choice of virtual crossings irrelevant. *Virtual isotopy is the same as the equivalence relation generated on the collection of oriented Gauss codes by abstract Reidemeister moves on these codes.*

Figure 3 illustrates the two *forbidden moves*. Neither of these follows from Reidemeister moves plus detour move, and indeed it is not hard to construct examples of virtual knots that are non-trivial, but will become unknotted on the application of one or both of the forbidden moves. The forbidden moves change the structure of the Gauss code and, if desired, must be considered separately from the virtual knot theory proper.

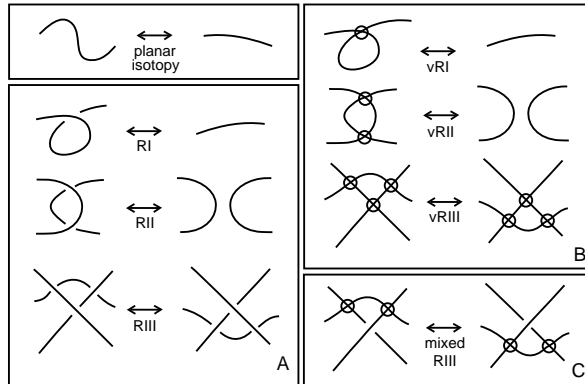


Figure 1: Moves

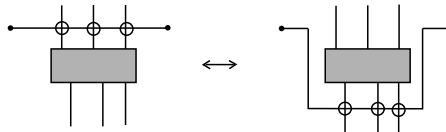


Figure 2: Detour Move

2.1 Interpretation of Virtuals Links as Stable Classes of Links in Thickened Surfaces

There is a useful topological interpretation [28, 30] for virtual knot theory in terms of embeddings of links in thickened surfaces. Regard each virtual crossing as a shorthand for a detour of one of the arcs in the crossing through a 1-handle that has been attached to the 2-sphere of the original diagram. By interpreting each virtual crossing in this way, we obtain an embedding of a collection of circles into a thickened surface $S_g \times R$ where g is the number of virtual crossings in the original diagram L , S_g is a compact oriented surface of genus g and R denotes the real line. We say that two such surface embeddings are *stably equivalent* if one can be obtained from another by isotopy in the thickened surfaces, homeomorphisms of the surfaces and the addition or subtraction of empty handles (i.e. the knot does not go through the handle).

We have the

Theorem 1 [28, 13, 30, 2]. *Two virtual link diagrams are isotopic if and only if their corresponding surface embeddings are stably equivalent.*

The reader will find more information about this correspondence [28, 13] in other papers by the author and in the literature of virtual knot theory.



Figure 3: Forbidden Moves

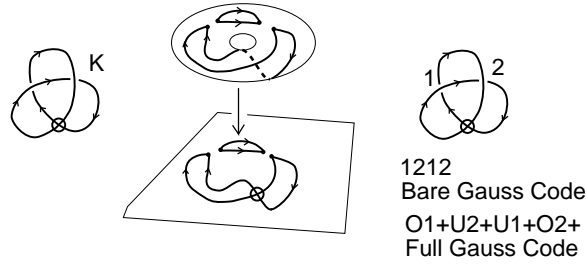


Figure 4: **Surface Representation**

2.2 Review of the Bracket Polynomial for Virtual Knots

In this section we recall how the bracket state summation model [14] for the Jones polynomial is defined for virtual knots and links.

The bracket polynomial [14] model for the Jones polynomial [21, 22, 23, 42] is usually described by the expansion

$$\langle \diagdown \rangle = A \langle \diagup \rangle + A^{-1} \langle \rangle \langle \rangle \quad (1)$$

and we have

$$\langle K \bigcirc \rangle = (-A^2 - A^{-2}) \langle K \rangle \quad (2)$$

$$\langle \diagup \rangle = (-A^3) \langle \smile \rangle \quad (3)$$

$$\langle \diagdown \rangle = (-A^{-3}) \langle \smile \rangle \quad (4)$$

We call a diagram in the plane *purely virtual* if the only crossings in the diagram are virtual crossings. Each purely virtual diagram is equivalent by the virtual moves to a disjoint collection of circles in the plane.

A state S of a link diagram K is obtained by choosing a smoothing for each crossing in the diagram and labelling that smoothing with either A or A^{-1} according to the convention indicated in the bracket expansion above. Then, given a state S , one has the evaluation $\langle K | S \rangle$ equal to the product of the labels at the smoothings, and one has the evaluation $\|S\|$ equal to the number of loops in the state (the smoothings produce purely virtual diagrams). One then has the formula

$$\langle K \rangle = \sum_S \langle K | S \rangle d^{\|S\|-1}$$

where the summation runs over the states S of the diagram K , and $d = -A^2 - A^{-2}$. This state summation is invariant under all classical and virtual moves except the first Reidemeister move. The bracket polynomial is normalized to an invariant $f_K(A)$ of all the moves by the formula $f_K(A) = (-A^3)^{-w(K)} \langle K \rangle$ where $w(K)$ is the writhe of the (now) oriented diagram K . The writhe is the sum of the orientation signs (± 1) of the crossings of the diagram. The Jones polynomial, $V_K(t)$ is given in terms of this model by the formula

$$V_K(t) = f_K(t^{-1/4}).$$

This definition is a direct generalization to the virtual category of the state sum model for the original Jones polynomial. It is straightforward to verify the invariances stated above. In this way one has the Jones polynomial for virtual knots and links.

We have [30] the

Theorem. *To each non-trivial classical knot diagram of one component K there is a corresponding non-trivial virtual knot diagram $Virt(K)$ with unit Jones polynomial.*

The main ideas behind this Theorem are indicated in Figure 5 and Figure 6. In Figure 5 we indicate the virtualization operation that replaces a classical crossing by using two virtual crossings and changing the implicit orientation of the classical crossing. We also show how the bracket polynomial sees this operation as though the crossing had been switched in the classical knot. Thus, if we virtualize as set of classical crossings whose switching will unknot the knot, then the virtualized knot will have unit Jones polynomial. On the other hand, the virtualization is invisible to the quandle, as shown in Figure 6. This implies (by properties of the quandle) that virtual knots obtained in this way from classical non-trivial knots will themselves be non-trivial.

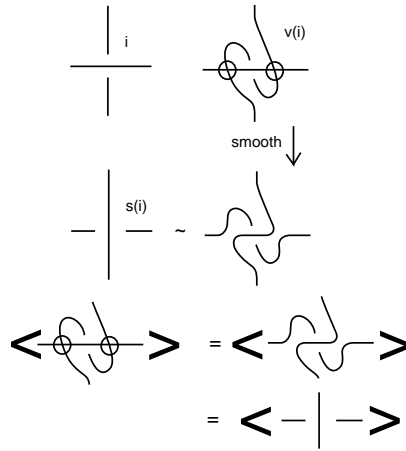


Figure 5: **Virtualizing a Crossing and Crossing Switches**

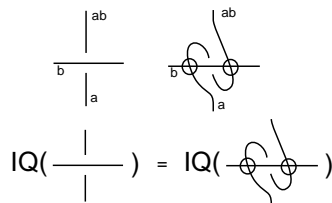


Figure 6: **Quandle Invariance Under Virtualization**

It is an open problem whether there are classical knots (actually knotted) having unit Jones polynomial. (There are linked links whose linkedness is unseen [4] by the Jones polynomial.) We do know, however, that the knots $Virt(K)$ produced by this Theorem for non-trivial classical knots K are never isotopic to a classical knot. Such examples are guaranteed to be non-trivial, and are not classical [3].

2.3 Parity and Odd Writhe

Parity is an important theme in virtual knot theory and figures in many investigations of this subject. In a virtual knot diagram there can be both even and odd crossings. A crossing is *odd* if it flanks an odd number of symbols in the Gauss code of the diagram. A crossing is *even* if it flanks an even number of symbols in the Gauss code of the diagram. For example, in Figure 4 we illustrate the virtual knot K with bare Gauss code 1212. Both crossings in the diagram K are odd. In any classical knot diagram all crossings are even.

In [33] we introduced the *odd writhe* $J(K)$ for any virtual diagram K . $J(K)$ is the sum of the signs of the odd crossings. Classical diagrams have zero odd writhe. Thus if $J(K)$ is non-zero, then K is not equivalent to any classical knot. For the mirror image K^* of any diagram K , we have the formula $J(K^*) = -J(K)$. Thus, when $J(K) \neq 0$, we know that the knot K is not classical and not equivalent to its mirror image. Parity does all the work in this simple invariant. For example, if K is the virtual knot in Figure 4, then we have $J(K) = 2$. Thus K , the simplest virtual knot, is non-classical and it is chiral (inequivalent to its mirror image.)

In Section 4 of this paper we will examine a generalization of the odd writhe to a polynomial invariant of virtual knots (the affine index polynomial [36]) and we shall see how these invariants behave under cobordism and concordance of virtual knots, as described in Section 3.

3 Virtual Knot Cobordism

Definition. Two oriented knots or links K and K' are *virtually cobordant* if one may be obtained from the other by a sequence of virtual isotopies (Reidemeister moves plus detour moves) plus births, deaths and oriented saddle points, as illustrated in Figure 7. A *birth* is the introduction into the diagram of an isolated unknotted circle. A *death* is the removal from the diagram of an isolated unknotted circle. A saddle point move results from bringing oppositely oriented arcs into proximity and resmoothing the resulting site to obtain two new oppositely oriented arcs. See the Figure for an illustration of the process. Figure 7 also illustrates the *schema* of surfaces that are generated by cobordism process. These are abstract surfaces with well defined genus in terms of the sequence of steps in the cobordism. In the Figure we illustrate two examples of genus zero, and one example of genus 1. We say that a cobordism has genus g if its schema has that genus. Two knots are *cocordant* if there is a cobordism of genus zero connecting them. A virtual knot is said to be a *slice* knot if it is virtually concordant to the unknot, or equivalently if it is virtually concordant to the empty knot (The unknot is concordant to the empty knot via one death.). As we shall see below, *every virtual knot or link is concordant to the unknot*. Another way to say this, is to say that there is a *virtual surface* (schema) whose boundary is the given virtual knot. The reader should note that when we speak of a virtual surface, we mean a surface schema that is generated by saddle moves, maxima and minima as describe above.

Definition. We define the *four-ball genus* $g_4(K)$ of a virtual knot or link K to be the least genus among all virtual surfaces obtained by virtual cobordism that bound K . As we shall see below, there is a simple upper bound on the four-ball genus for any virtual knot or link and a definite result for the four-ball genus of positive virtual knots [3]. Note that in this definition of four-ball genus we have not made reference to an embedding of the surface in the four-ball D^4 . The surface constructed by a virtual cobordism is, for this paper, an abstract surface with a well-defined genus. This same surface can be given the structure of virtual surface diagram analogous to a virtual knot or link diagram (see [40]) but we will not discuss this aspect of virtual surfaces in the present paper. Note that virtual slice knots are virtual knots K with $g_4(K) = 0$.

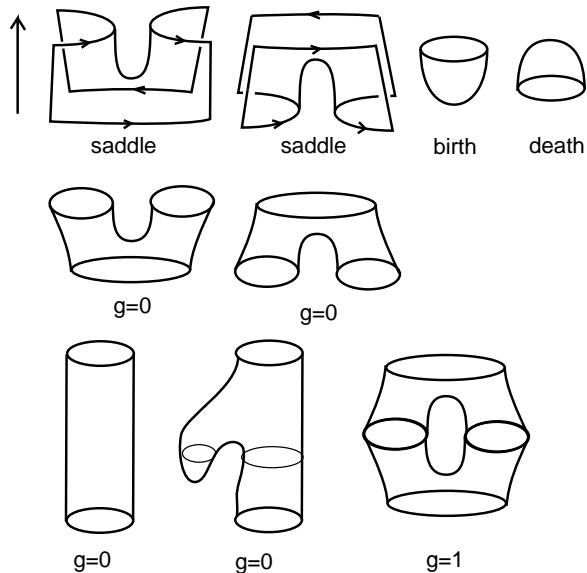


Figure 7: **Saddles, Births and Deaths**

In Figure 8 we illustrate the *virtual stevedore's knot*, VS and show that it is a slice knot in the sense of the above definition. This figure illustrates how the surface schema whose boundary in the virtual stevedore is evolved via the saddle point that produces two virtually unlinked curves that are isotopic to a pair of curves that can undergo deaths to produce the genus zero slicing surface. We will use this example to illustrate our theory of virtual knot cobordism, and the questions that we are investigating. In Figure 10 we show an equivalent version (See Figure 9) of the virtual stevedore's knot that is reminiscent of a ribbon diagram for classical knots, and we see that there is a single saddle point move that slices this version of the virtual stevedore.

In Figure 11 will illustrate a connected sum of a virtual knot K and its *vertical mirror image* $K^!$. The vertical mirror image is obtained by reflecting the diagram in a plane perpendicular to the plane of the diagram *and reversing the orientation of the resulting diagram*. We indicate this particular connected sum by $K \# K^!$. While connected sum of virtual knots is not in general defined except by a diagrammatic choice, we do have a diagrammatic definition of this connected sum and it is the case that $K \# K^!$ is a *slice knot for any virtual diagram* K . The idea behind the proof of this statement is illustrated in Figure 12. Saddle points can be made by pairing arcs across the mirror and the diagram resolves into a collection of virtual trivial circles. We omit the detailed proof of this fact about virtual concordance. This result is a direct generalization of the corresponding result for classical knots and links [5].

3.1 Spanning Surfaces for Knots and Virtual Knots and the Four-Ball Genus of Positive Virtual Knots

It is a well-known that every oriented classical knot or link bounds an embedded orientable surface in three-space. A representative surface of this kind can be obtained by the algorithm due to Seifert (See [10, 9, 24]). We have illustrated Seifert's algorithm for a trefoil diagram in Figure 13. The algorithm

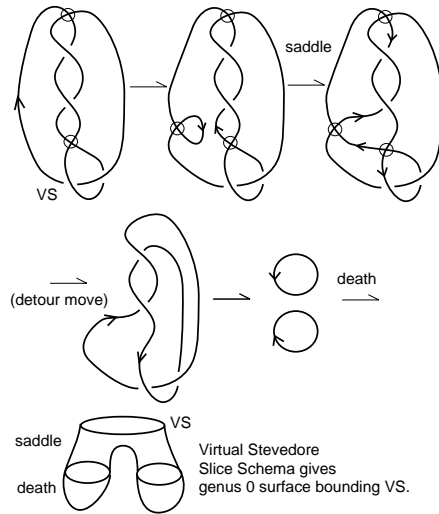


Figure 8: **Virtual Stevedore is Slice**

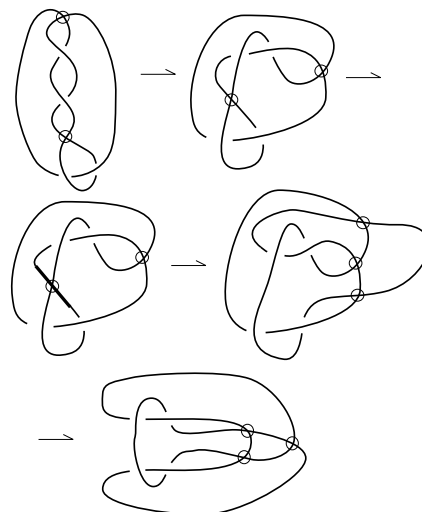


Figure 9: **Converting Virtual Stevedore to a “Ribbon Diagram”**

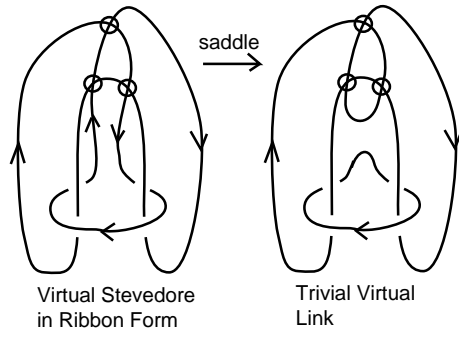


Figure 10: **Ribbon Version of Virtual Stevedore**

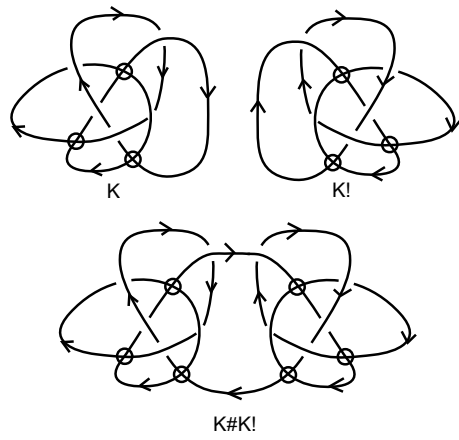


Figure 11: Vertical Mirror Image

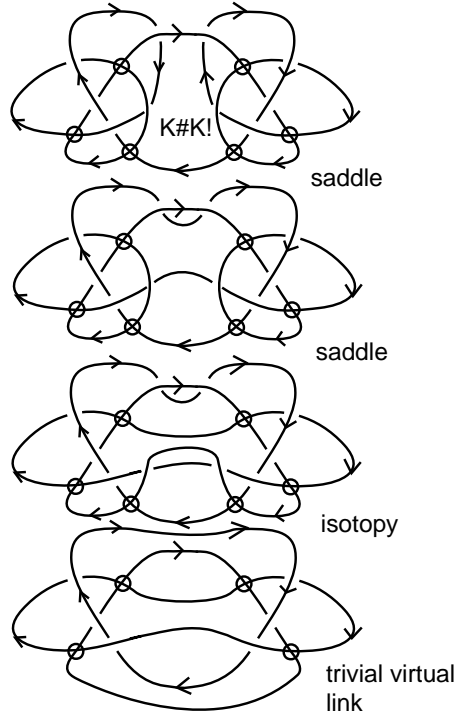


Figure 12: Connected Sum With Vertical Mirror Image is Slice

proceeds as follows: At each oriented crossing in a given diagram K , smooth that crossing in the oriented manner (reconnecting the arcs locally so that the crossing disappears and the connections respect the orientation). The result of this operation is a collection of oriented simple closed curves in the plane, usually called the *Seifert circles*. To form the *Seifert surface* $F(K)$ for the diagram K , attach disjoint discs to each of the Seifert circles, and connect these discs to one another by local half-twisted bands at the sites of the smoothing of the diagram. This process is indicated in the Figure 13. In that figure we have not completed the illustration of the outer disc.

It is important to observe that we can calculate the genus of the resulting surface quite easily from the combinatorics of the classical knot diagram K . For purposes of simplicity, we shall assume that we are dealing with a knot diagram (one boundary component) and leave the case of links to the reader. We then have the

Lemma. Let K be a classical knot diagram with n crossings and r Seifert circles. then the genus of the Seifert Surface $F(K)$ is given by the formula

$$g(F(K)) = (1/2)(-r + n + 1).$$

Proof. The surface $F(K)$, as described prior to the statement of the Lemma, retracts to a cell complex consisting of the projected graph of the knot diagram with two-cells attached to each cycle in the graph that corresponds to a Seifert circle. Thus we have that the Euler characteristic of this surface is given the the formula

$$\chi(F(K)) = n - e + r$$

where n , the number of crossings in the diagram, is the number of zero-cells, e is the number of one-cells (edges) in the projected diagram (from node to node), and r is the number of Seifert circles as

these are in correspondence with the two-cells. However, we know that $4n = 2e$ since there are four edges locally incident to each crossing. Thus,

$$\chi(F(K)) = -n + r.$$

Furthermore, we have that $\chi(F(K)) = 1 - 2g(F(K))$, since this surface has a single boundary component and is orientable. From this it follows that $1 - 2g(F(K)) = -n + r$, and hence

$$g(F(K)) = (1/2)(-r + n + 1).$$

This completes the proof. //

We now observe that *for any classical knot K , there is a surface bounding that knot in the four-ball that is homeomorphic to the Seifert surface*. One can construct this surface by pushing the Seifert surface into the four-ball keeping it fixed along the boundary. We will give here a different description of this surface as indicated in Figure 14. In that figure we *perform a saddle point transformation at every crossing of the diagram*. The result is a collection of unknotted and unlinked curves. By our interpretation of surfaces in the four-ball obtained by saddle moves and isotopies, we can then bound each of these curves by discs (via deaths of circles) and obtain a surface $S(K)$ embedded in the four-ball with boundary K . As the reader can easily see, the curves produced by the saddle transformations are in one-to-one correspondence with the Seifert circles for K , and it easy to verify that $S(K)$ is homeomorphic with the Seifert surface $F(K)$. Thus we know that $g(S(K)) = (1/2)(-r + n + 1)$. In fact the same argument that we used to analyze the genus of the Seifert surface applies directly to the construction of $S(K)$ via saddles and minima.

Now the stage is set for generalizing the Seifert surface to a surface $S(K)$ for virtual knots K . View Figure 15 and Figure 16. In these figures we have performed a saddle transformation at each classical crossing of a virtual knot K . The result is a collection of unknotted curves that are isotopic (by the first classical Reidemeister move) to curves with only virtual crossings. Once the first Reidemeister moves are performed, these curves are identical with the *virtual Seifert circles* obtained from the diagram K by smoothing all of its classical crossings. We can then Isotope these circles into a disjoint collection of circles (since they have no classical crossings) and cap them with discs in the four-ball. The result is a virtual surface $S(K)$ whose boundary is the given virtual knot K . We will use the terminology *virtual surface in the four-ball* for this surface schema. In the case of a virtual slice knot, we have that the knot bounds a virtual surface of genus zero. But with this construction we have proved the

Lemma. Let K be a virtual knot, then the virtual Seifert surface $S(K)$ constructed above has genus given by the formula

$$g(S(K)) = (1/2)(-r + n + 1)$$

where r is the number of virtual Seifert circles in the diagram K and n is the number of classical crossings in the diagram K .

Proof. The proof follows by the same argument that we already gave in the classical case. Here the projected virtual diagram gives a four-regular graph G (not necessarily planar) whose nodes are in one-to-one correspondence with the classical crossings of K . The edges of G are in one-to-one correspondence with the edges in the diagram that extend from one classical crossing to the next. We regard G as an abstract graph so the the virtual crossings disappear. The argument then goes over verbatim in the sense that G with two-cells attached to the virtual Seifert circles is a retract of the surface $S(K)$ constructed by cobordism. The counting argument for the genus is identical to the classical case. This completes the proof. //

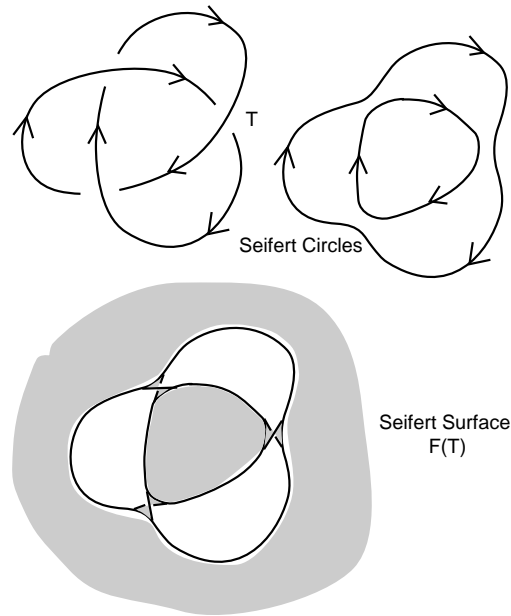


Figure 13: **Classical Seifert Surface**

Remark. For the virtual stevedore in Figure 16 we have the interesting phenomenon that there is a lower genus surface (genus zero as we have already seen in Section 2) than can be produced by cobordism using the virtual Seifert surface. In that same figure we have illustrated a diagram D with the same projected diagram as the virtual stevedore, but D has all positive crossings. In this case we can prove [3] that there is no virtual surface for this diagram D of four-ball genus less than 1. In fact, we have the following result which is proved in [3]. This Theorem is a generalization of a corresponding result for classical knots due to Rasmussen [20].

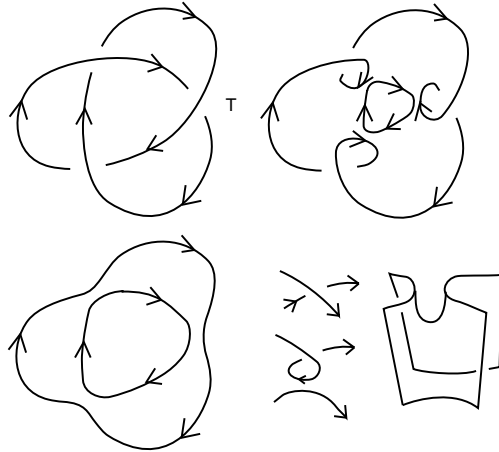
Remark. Note that it follows from this discussion that if a diagram K' is obtained from a diagram K by replacing a crossing in K by its oriented smoothing, then K' is cobordant to K via a single saddle point move. We will use this observation repeatedly in the rest of the paper.

Theorem on Four-Ball Genus for Positive Virtual Knots [3]. Let K be a positive virtual knot (all classical crossings in K are positive), then the four-ball genus $g_4(K)$ is given by the formula

$$g_4(K) = (1/2)(-r + n + 1) = g(S(K))$$

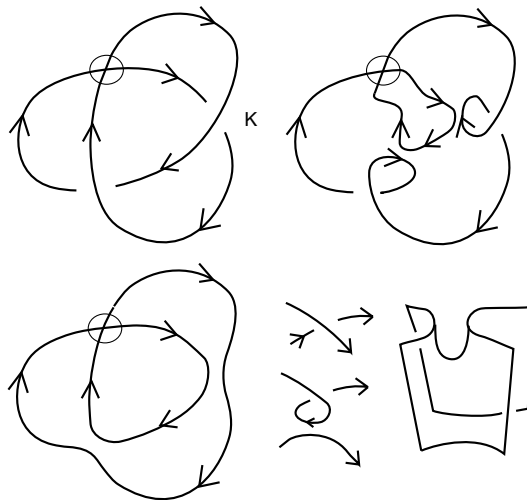
where r is the number of virtual Seifert circles in the diagram K and n is the number of classical crossings in this diagram. In other words, the virtual Seifert surface for K represents its minimal four-ball genus.

Discussion. This Theorem is proved by using a generalization of integral Khovanov homology to virtual knot theory originally devised by Manturov [32]. In [3] we reformulate this theory and show that it generalizes to the Lee homology theory (a variant of Khovanov homology) as well. With this theorem, we know the genus for an infinite class of virtual knots and can begin the deeper exploration of genus for non-positive virtual knots and links.



Every classical knot diagram bounds a surface in the four-ball whose genus is equal to the genus of its Seifert Surface.

Figure 14: **Classical Cobordism Surface**



Seifert Circle(s) for K

Every virtual diagram K bounds a virtual orientable surface of genus $g = (1/2)(-r + n + 1)$ where r is the number of Seifert circles, and n is the number of classical crossings in K.

This virtual surface is the cobordism Seifert surface when K is classical.

Figure 15: **Virtual Cobordism Seifert Surface**

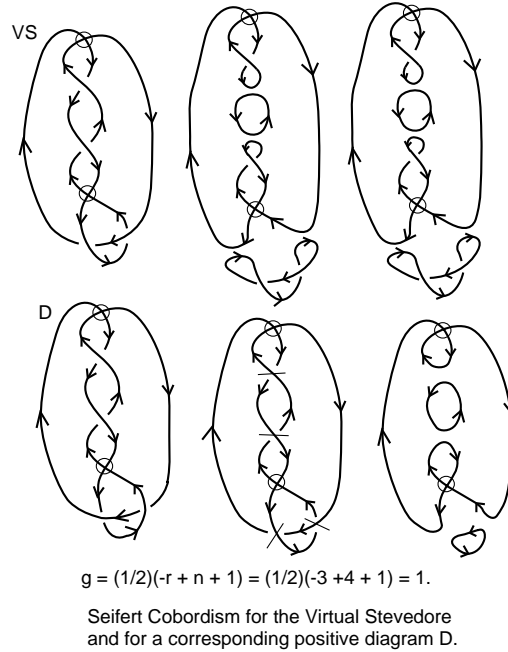


Figure 16: **Virtual Stevedore Cobordism Seifert Surface**

3.2 Properties of the Virtual Stevedore's Knot

See [16] for the details behind the following facts. We prove that VS is not classical by showing that it is represented on a surface of genus one and no smaller. The technique for finding this surface genus for the virtual stevedore is to use the bracket expansion on a toral representative of VS and examine the structure of the state loops on that surface. An analysis of the homology classes of the state loops shows that the knot cannot be isotoped off the handle structure of the torus. See [11, 26] for more information about using the surface bracket. The virtual stevedore has the same bracket polynomial as the classical figure eight knot. This calculation shows that VS is not a connected sum of two virtual knots. Thus we know that VS is a non-trivial example of a virtual slice knot.

4 The Affine Index Polynomial Invariant

We define a polynomial invariant of concordance of virtual knots by first describing how to calculate the polynomial, then proving invariance under virtual link equivalence and then proving invariance under concordance. Calculation begins with a flat oriented virtual knot diagram (the classical crossings in a flat diagram do not have choices made for over or under). An *arc* of a flat diagram is an edge of the 4-regular graph that it represents. That is, an edge extends from one classical node to the next in orientation order. An arc may have many virtual crossings, but it begins at a classical node and ends at another classical node. We label each arc c in the diagram with an integer $\lambda(c)$ so that an arc that meets a classical node and crosses to the left increases the label by one, while an arc that meets a classical node and crosses to the right decreases the label by one. See Figure 17 for an illustration of this rule. We will prove that such integer labelling can always be done for any virtual or classical link diagram. In a virtual diagram the labeling is unchanged at a virtual crossing, as indicated in Figure 17. One

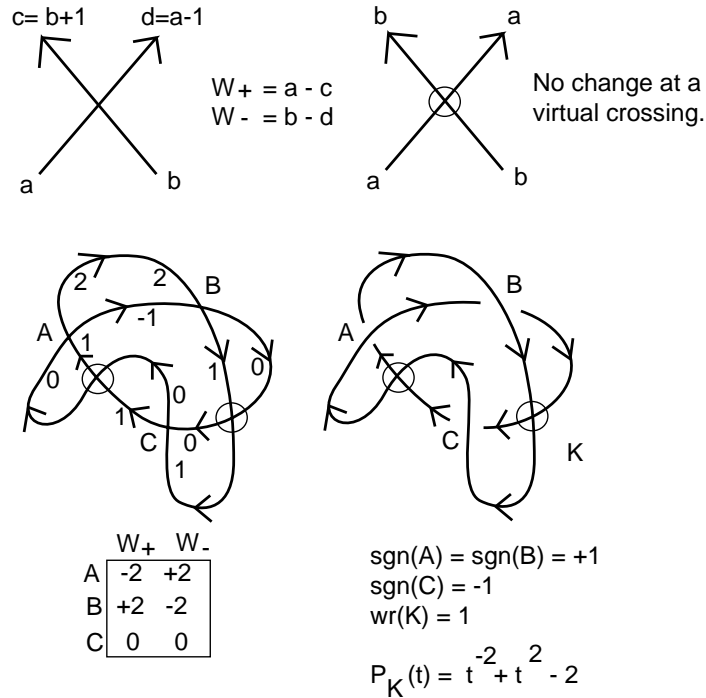


Figure 17: Labeled Flat Crossing and Example 1

can start by choosing some arc to have an arbitrary integer label, and then proceed along the diagram labelling all the arcs via this crossing rule. We call such an integer labelling of a diagram an *affine labeling* of the diagram and sometimes just a *labeling* of the diagram.

Remark. We discuss the algebraic background to this invariant in [36].

Given a labeled flat diagram we define two numbers at each classical node c : $W_-(c)$ and $W_+(c)$ as shown in Figure 1. If we have a labeled classical node with left incoming arc a and right incoming arc b then the right outgoing arc is labeled $a - 1$ and the left outgoing arc is labeled $b + 1$ as shown in Figure 17. We then define $W_+(c) = a - (b + 1)$ and $W_-(c) = b - (a - 1)$. Note that $W_-(c) = -W_+(c)$ in all cases.

Definition. Given a crossing c in a diagram K , we let $\text{sgn}(c)$ denote the sign of the crossing. The sign of the crossing is plus or minus one according to the convention shown in Figure 18. The *writhe*,

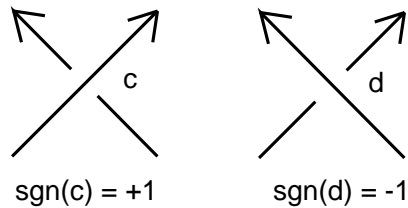


Figure 18: Crossing Signs

$wr(K)$, of the diagram K is the sum of the signs of all its crossings. For a virtual link diagram, labeled in the integers according to the scheme above, and a crossing c in the diagram, define $W_K(c)$ by the equation

$$W_K(c) = W_{sgn(c)}(c)$$

where $W_{sgn(c)}(c)$ refers to the underlying flat diagram for K . Thus $W_K(c)$ is $W_{\pm}(c)$ according as the sign of the crossing is plus or minus. We shall often indicate the weight of a crossing c in a knot diagram K by $W(c)$ rather than $W_K(c)$.

Let K be a virtual knot diagram. Define the *Affine Index Polynomial* of K by the equation

$$P_K = \sum_c sgn(c)(t^{W_K(c)} - 1) = \sum_c sgn(c)t^{W_K(c)} - wr(K)$$

where the summation is over all classical crossings in the virtual knot diagram K . The Laurent polynomial P_K is a highly non-trivial invariant of virtual knots. Note that we can rewrite this definition as follows:

$$P_K = \sum_{n=1}^{\infty} wr_n(K)(t^n - 1)$$

where

$$wr_n(K) = \sum_{c:W_K(c)=n} sgn(c).$$

We can think of these numbers $wr_n(K)$ as special writhes for the virtual knot diagram, similar in spirit to the odd writhe. Each $wr_n(K)$ for $n = 1, 2, \dots$ is an invariant of the virtual knot K . Note also that a crossing c in K is odd (by our previous definition) if and only if $W_K(c)$ is odd. Thus, if $J(K)$ denotes the odd writhe of K , then

$$J(K) = \sum_{c:W_K(c) \text{ odd}} sgn(c) = \sum_{n \text{ odd}} wr_n(K).$$

Remark. In Figure 17 we show the computation of the weights for a given flat diagram and the computation of the polynomial for a virtual knot K with this underlying diagram. The knot K is an example of a virtual knot with unit Jones polynomial. The polynomial P_K for this knot has the value

$$P_K = t^{-2} + t^2 - 2,$$

showing that this knot is not isotopic to a classical knot.

5 Invariance of $P_K(t)$.

In order to show the invariance and well-definedness of $P_K(t)$ we must first show the existence of affine labelings of flat virtual knot diagrams. We do this by showing that any virtual knot diagram K that overlies a given flat diagram D can be so labeled.

Proposition. Any flat virtual knot diagram has an affine labelling.

Proof. This proposition is proved in [36]. The main point is that on traversing the entire diagram, one goes through each crossing twice. The combination of these two operations results in a total change of zero. Hence, whatever label one begins with, the return label after a complete circuit of a diagram component will be the same as the start label.

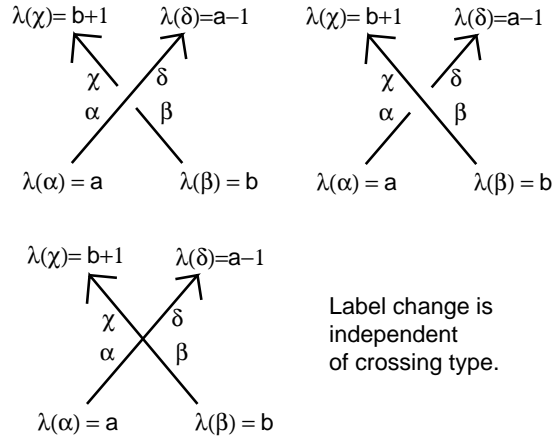


Figure 19: Labels for Crossings

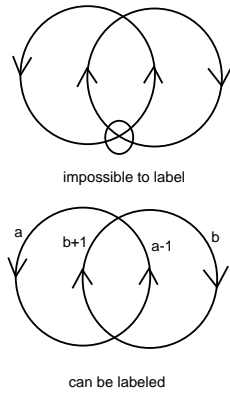


Figure 20: Possible and Impossible Labels for Links

Remark. Not all multicomponent virtual diagrams can be labeled. See Figure 20 for such an example. We call a multi-component diagram D *compatible* if every component of the diagram has algebraic intersection number zero (taking signed intersection numbers in the plane) with the other components in D . We observe the following

Lemma. Let D be a multi-component virtual diagram. Then D can be given an affine labeling if and only if it is compatible.

Proof. In any traverse of a given component of D one will meet external crossings each once, and increment or decrement the labeling according as the crossing has positive or negative sign with respect to this component. Self-crossings are met twice, once as an increment and once as a decrement. Thus the total traverse will not change the initial label if and only if the algebraic intersection number of the given component with the rest of the diagram is zero. Since this must hold for each component of the diagram D , we conclude that D can be labeled if and only if D is compatible. //

If we follow the algorithm described in Figure 17 to compute a labeling, using a different starting

value, the resulting labeling will differ from the first labeling by a constant integer at every label. Since the polynomial is defined in terms of the differences $W_{\pm}(c)$ at each classical crossing c of K , it follows that the weights W_{\pm} as described above are well-defined.

We can now state a result about the weights. See [36] for the proof. Let \bar{K} denote the diagram obtained by reversing the orientation of K and let K^* denote the diagram obtained by switching all the crossings of K . \bar{K} is called the *reverse* of K , and K^* is called the *flat mirror image* of K . We let K^\dagger denote the *vertical mirror image* of K as shown in Figure 11. The vertical mirror image is obtained by reflecting the diagram in a plane perpendicular to the plane of the diagram.

Proposition. Let K be a virtual knot diagram and $W_{\pm}(c)$ the crossing weights as defined in section 1 and above. If α is an arc of K , let $\bar{\alpha}$ denote the corresponding arc of \bar{K} , the result of reversing the orientation of K .

1. Let c be a crossing of K and let \bar{c} denote the corresponding crossing of \bar{K} , then $W(\bar{c}) = -W(c)$. Hence,

$$P_{\bar{K}}(t) = P_K(t^{-1}).$$

Similarly, for the flat mirror image we have

$$P_{K^*}(t) = -P_K(t^{-1}),$$

and for the vertical mirror image

$$P_{K^\dagger}(t) = -P_K(t).$$

Thus this invariant changes t to t^{-1} when the orientation of the knot is reversed, and it changes global sign and t to t^{-1} when the knot is replaced by its flat mirror image.

2. If K is a classical knot diagram, then for each crossing c in K , $W(c) = 0$ and $P_K(t) = 0$.
3. If $K\sharp L$ denotes a connected sum (the diagrams are joined by removing an arc from each, and connecting them) of K and L , then

$$P_{K\sharp L} = P_K + P_L.$$

Thus, if $K\sharp K^\dagger$ denotes a connected sum of a virtual knot with its vertical mirror image (see Figure 11), then it follows from the above that

$$P_{K\sharp K^\dagger} = P_K - P_{K^\dagger} = 0.$$

We will now prove the invariance of $P_K(t)$ under virtual isotopy. The reader will recall that virtual isotopy consists in the classical Reidemeister moves plus virtual moves that are all generated by one generic detour move. The (unoriented) virtual isotopy moves are illustrated in Figure 1 and Figure 2. In Figure 24 and Figure 25 we show the relevant information for verifying that $P_K(t)$ is an invariant of oriented virtual isotopy.

Theorem. Let K be a virtual knot diagram. Then the polynomial $P_K(t)$ is invariant under oriented virtual isotopy and is hence an invariant of virtual knots.

Proof. Note that the definition of $P_K(t)$ makes it independent of the moves in Figure 1 involving virtual crossings. The labeling algorithm is independent of the purely virtual moves and consequently the polynomial is invariant under them. Thus we need only verify invariance under the standard oriented Reidemeister moves, shown as box A in Figure 1. Note that the affine coloring is uniquely inherited under the Reidemeister moves, and thus we only have to check the local changes in the coloring in relation to given types of move. Since we wish to verify invariance under oriented Reidemeister moves, we use the well-known fact (see [24] page 81) that it is sufficient to verify invariance under type I moves, two orientations of type II moves and the single instance of the type III move where

there is a non-cyclic triangle in the center of the pattern and all the crossings have the same type (say positive). In Figure 24 we give the relevant information for the moves of type I and II. For the type I move, we see that the weight $W_{\pm}(z)$ equals 0. This means that the contribution of a diagram with a type I move at a crossing z is equal to $sgn(z)$. Since this is subtracted by the writhe $wr(K)$ in the formula $P_K = \sum_c sgn(c)t^{W_K(c)} - wr(K)$, we see that the polynomial is invariant under move I. For move II there are two cases or orientation as shown in the Figure 24. In each case, the move is available when the crossings have opposite sign. The calculation shown in the figure proves that when the crossings have opposite sign, the weights of the crossings are identical. Thus the sum of these two crossing contributions cancels out in the polynomial both in the t -terms and in the writhe term. Therefore the polynomial is invariant under the II move. Finally, we examine the III move via the information in Figure 25. Here we assume that all three crossings are positive. The labels are calculated from flat versions of the move. We see that the resulting weights are simply permuted and the signs of the crossings remain unchanged. Thus the polynomial is invariant under move III. This completes the proof of the theorem. //

Generalization of the Affine Index Polynomial from Knots to Links. We are now in a position to generalize the invariant $P_K(t)$ to cases of virtual and classical link diagrams. Special link diagrams can be affine colored according to our rules. For example, view Figure 21 to see a labelling of the classical Hopf link. Before analyzing this figure, consider the proof we have given for the invariance of the polynomial $P_K(t)$. Affine coloring is uniquely inherited under Reidemeister moves and the weights at the three crossings of the third Reidemeister move are permuted under the move. These properties are true for the polynomial that we would write for any affine-colored link. Thus we can conclude that *if we are given pair (L, C) where L is a link diagram and C is an affine-coloring of this diagram, then the polynomial $P_L(t)$, defined just as before, is an invariant of the pair (L, C) where a Reidemeister move applied to (L, C) produces (L', C') where L' is the diagram obtained from L by the move, and C' is the coloring uniquely obtained from C by the move. The resulting polynomial is an invariant of the link itself.*

Now go back to Figure 21 and note that we have given arbitrary labels p and q to arcs on the two components and obtained weights of the form $-N - 1$ and $-N + 1$ where $N = p - q$. If we regard N as an integer variable in the polynomial $P_H = t^{-N-1} + t^{-N+1} - 2$ (H is a positive Hopf link.), then this polynomial is an invariant of the link. This can be verified by applying Reidemeister moves to the link and showing that the value of N is preserved.

In working with the invariant for a link we choose an *algebraic* starting value for each component of the link, using a different algebraic symbol for each component. It is convenient in displaying the weights to use new variables corresponding to the differences between algebraic labels. Thus in Figure 22 we have a two component virtual link with labels a and b for each component and we define $N = a - b$. At a crossing between two components the weights will be expressed uniquely in terms of N (the difference between their algebraic labels). The invariant polynomial for the link has algebraic exponents involving these differences. In Figure 22 the polynomial is $P_K = t^{N-1} + t^{-N} + t - 3$.

In Figure 23 we illustrate a link L that is a virtual Borromean rings. No two components are linked but the triple is linked. The algebraically weighted affine index polynomial detects the linkedness of these rings. Note that in this case we have two algebraic exponents N and M . We leave it to the reader to examine Figure 23 for more details about this example.

We have defined *compatibility* of multi-component diagrams above and proved that a multi-component diagram can be affine labeled if and only if it is compatible. Therefore compatible links have affine index polynomials. Just as we have remarked, such polynomials will in general have exponents that are new variables and that can be specialized to polynomials of labeled pairs. It is useful to have both

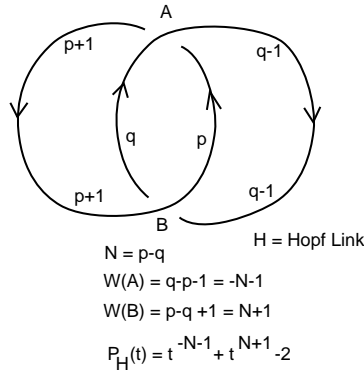


Figure 21: Invariant for the Hopf Link

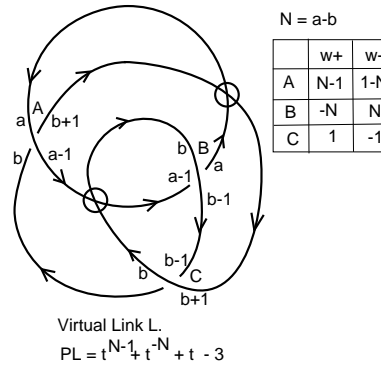


Figure 22: Affine Index Invariant of a Virtual Link

the absolute link invariants and the labeled pair invariants. We shall use both types of invariant in the discussion to follow.

6 Concordance Invariance of the Affine Index Polynomial

The main result of this section is the

Theorem. The affine index polynomial $P_K(t)$ is a concordance invariant of virtual knots K and compatible virtual links (the links for which the invariant is defined). In the case of links we use integral affine labelings for the link, just as in the case of knots and the genus zero concordance is restricted to one where all critical points can be paired in cancelling maxima and saddles and cancelling saddles and minima. Note that this condition is automatically satisfied in the case of concordance of knots.

Proof. Suppose that K is concordant to K' . Then there is a genus zero sequence of births deaths and saddles connecting K to K' . Genus zero implies that the core structure of this sequence is a tree of saddles, births and deaths. The genus zero surface can be seen as constructed from a sequence of

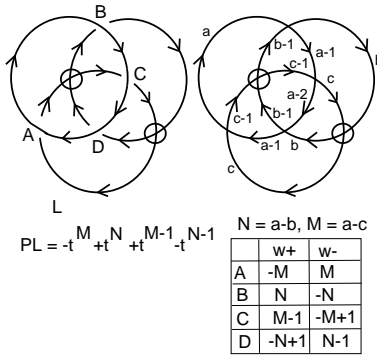


Figure 23: Affine Index Invariant of a Virtual Borromean Rings

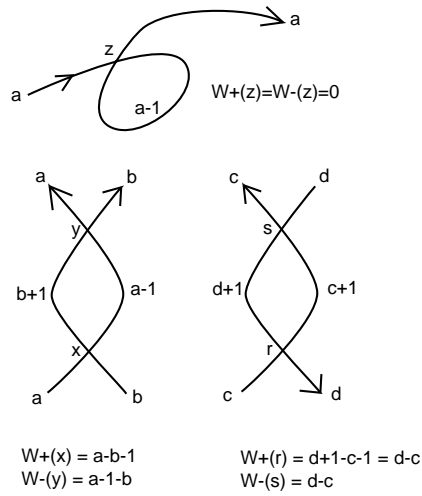


Figure 24: Reidemeister Moves 1 and 2

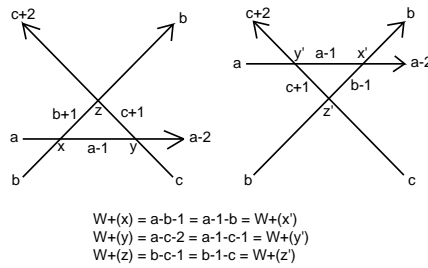


Figure 25: Reidemeister Move 3

pairings of births with saddles and saddles with deaths. In other words, the basic operation that constructs the concordance consists in the splitting off or amalgamation of a trivial knot with the body of the concordance via a birth and saddle or a saddle and a death. Thus we can consider an elementary genus zero concordance consisting in a virtual knot K and a trivial circle C disjoint from K such that the link diagram L consisting of the disjoint union of K and C undergoes virtual isotopy to a diagram D and one oriented saddle point move on D forms a new knot K' . It is sufficient to prove that $P_K = P_{K'}$. To prove this fact, note that by taking a constant labeling of C we have a defined polynomial P_L with $P_K = P_L$. Then L is isotopic to D and so by invariance of the affine index polynomial, $P_K = P_L = P_D$. At the place of the saddle point move there is a label a on the K component of D and a label b on the C component of D . We can add $a - b$ to the labels on all arcs of the C component of D and retain a legal coloring of D that does not change its polynomial evaluation (This is a general property of the labelings - they can always be shifted by a constant.). Thus we may assume that D is prepared with a labeling so that $P_K = P_D$ and the labels at the saddle point are the same. Then the saddle move can be performed and the new diagram K' inherits the same labeling. Hence $P_D = P_{K'}$. We have proved that $P_K = P_{K'}$. This completes the proof of the case of a birth followed by a saddle point. The remaining case is a saddle point followed by a death. In this case the link obtained after the saddle point inherits a labeling from the original knot and, given that the resulting link is isotopic to a disjoint union of a knot and a trivial circle, the argument proceeds as before. For links the criterion for the invariant to be defined is the existence of a labeling for the link diagram. Once we know that the labeling exists the above arguments apply equally well to the case of links. This completes the proof that the affine index polynomial is an invariant of concordance of virtual knots and links.//

Remark. In Figure 28 we illustrate an elementary concordance, as discussed in the proof above. The diagram K' is transformed by a single saddle point move to the diagram D , which is isotopic to a diagram that is the disjoint union of K and C where C is an unknotted circle. Letting C undergo death, we have a concordance from K' to K . We leave labeling this figure to the reader. It is clear that the crossings of the component of D that becomes C in the isotopy will have a total contribution of zero to the polynomial and that their contribution to D is identical to their contribution to K' . Thus we see directly in this case how $P_K = P_{K'}$. In Figure 29 we show the weight calculation for the first part of the concordance in the previous figure. Note that the total weight contribution to the affine index polynomial from the unknotted and unlinked component (after the saddle move) is zero. This is in accord with the proof of the Theorem.

Remark. Any virtual slice knot K will have $P_K(t) = 0$ since K is concordant to the unknot. In the case of the virtual stevedore knot, we see in Figure 26 that all the weights are zero. We can ask when a virtual knot will have all of its weights equal to zero. It is certainly not the case that any virtual slice knot will have null weights. For example, view Figure 27 where we show the knot $K \sharp K^1$ where K is the virtual trefoil, and K^1 denotes the vertical mirror image of K (the mirror is a plane perpendicular to the diagram plane). We know that $P_{K^1}(t) = -P_K(t)$ for any virtual knot K . And so $P_{K \sharp K^1} = 0$ for any virtual knot K . In fact, as remarked in the previous section, it is the case that $K \sharp K^1$ is virtually slice for any virtual knot K . In such examples it is often the case that P_K is non-trivial and so the diagram has canceling but non-null weights. This is the case in this specific example, where $P_K = t^{-1} + t - 2$.

We finish this paper with a process that applies to most examples of the affine index polynomial. Taking a knot or link diagram K with a labeling, some of the weights may be zero. At each crossing with weight zero, we can smooth the crossing to obtain a link L that is cobordant to K (recall that smoothing a crossing can be accomplished by one saddle move). Thus we can smooth all crossings with null weights and obtain a knot or link K' such that K is cobordant to K' , K' has only non-zero weights (or it is an unknot or unlink) and $P_K = P_{K'}$. This process of removing crossings and making

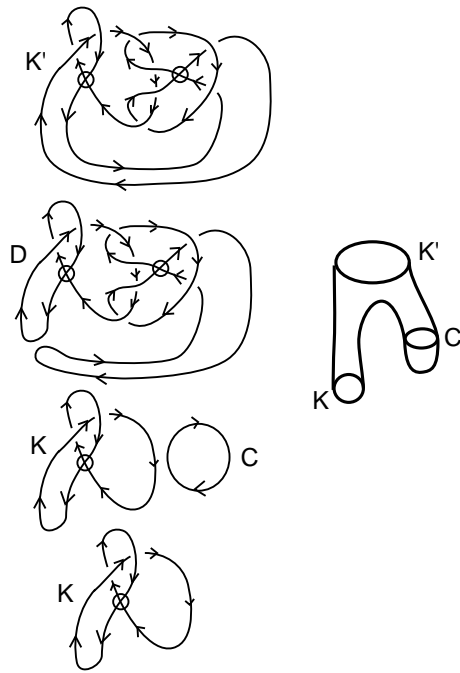


Figure 28: An Elementary Concordance between K and K'

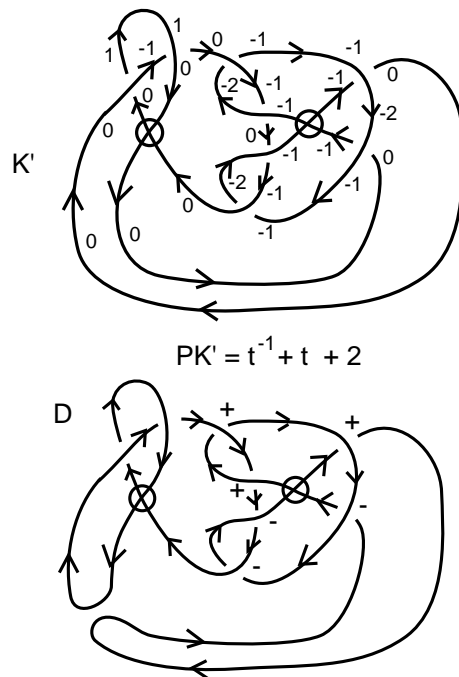


Figure 29: An Elementary Labeled Concordance

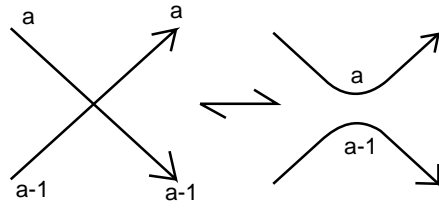


Figure 30: Basic Labeled Cobordism

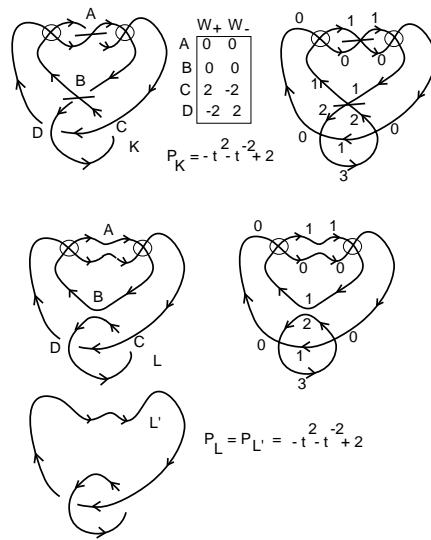


Figure 31: Labeled Cobordism of a Knot to a Link

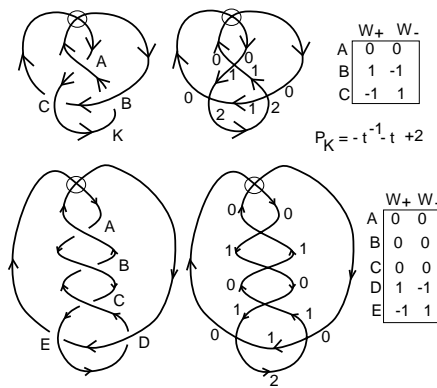


Figure 32: A Family of Virtual Knots with the Same Polynomial

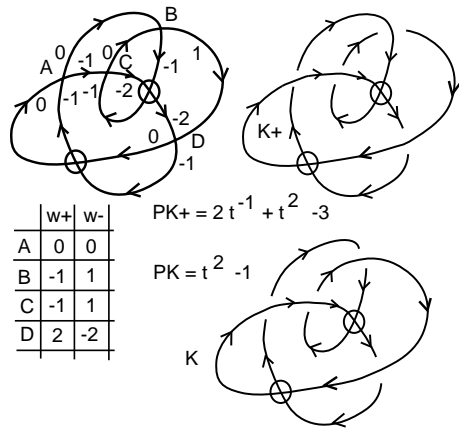
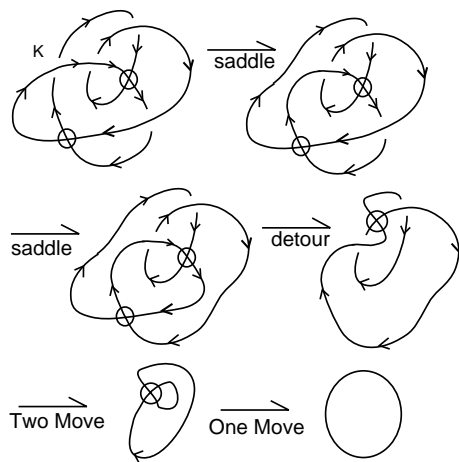


Figure 33: Polynomial Calculation for Two Knots



K bounds a virtual surface of genus one.

Figure 34: The Knot K has virtual genus one.

a cobordism that does not change the polynomial is particularly interesting in many examples. The link K' in its way, contains the core of the invariant for K and the remaining obstruction to making a concordance. Here are descriptions of some examples of this phenomenon.

1. In Figure 30 and Figure 31 we illustrate how the appearance of zeroes in the list of vertex weights for the polynomial can be used to produce labelled knots and links where the crossings with null weights have been smoothed. We will call the smoothing indicated in Figure 30 a *basic labeled cobordism*. Thus if a knot has crossings with null weights, then it is labeled cobordant to a link with only non-zero weights (or an empty set of weights). While not all links can be labeled, this form of cobordism does produce labeled links, and the Index Invariant can be extended to such links as indicated in Figure 21. Here we write down the most general labeling for the link, and then deduce a set of variable integer exponents for the polynomial invariant, as described in the previous section of this paper.
2. Figure 32 Illustrates an infinite family of virtual knots with the same Affine Index Polynomial. Note that all of them are labeled cobordant to the Hopf link diagram. They can all be distinguished from one another by the bracket polynomial.
3. In Figure 33 we illustrate the calculation of the affine index polynomial for two knots $K+$ and K . The knot $K+$ is positive and by our theorem on the genus of positive virtual knots, it has genus two. The knot K is obtained from $K+$ by switching one crossing. The affine index polynomial shows that it is not slice and Figure 34 shows that K bounds a genus one virtual surface. Thus we know, using the affine index polynomial, that K has genus equal to one.

References

- [1] H. Boden, M. Chrisman and R. Gaudreau. Virtual Knot Cobordism and Bounding the Silce Genus. arXiv:1708.05982v2, 26Dec2017.
- [2] J. Scott Carter, Seiichi Kamada, Masahico Saito. Stable Equivalence of Knots on Surfaces and Virtual Knot Cobordisms. math.GT/0008118
- [3] Heather A. Dye, Aaron Kaestner and Louis H. Kauffman, Khovanov homology, Lee homology and a Rasmussen invariant for virtual knots. J. Knot Theory Ramifications 26 (2017), no. 3, 1741001, 57 pp.
- [4] S. Eliahou, L. Kauffman and M. Thistlethwaite, Infinite families of links with trivial Jones polynomial, *Topology* **42**, 155-169.
- [5] R. H. Fox and J. W. Milnor, Singularities of 2-spheres in 4-space and cobordism of knots, Osaka J. Math. 3 (1966), pp. 257 - 267.
- [6] Ggmc, Neslihan; Kauffman, Louis H. New invariants of knotoids. European J. Combin. 65 (2017), 186229.
- [7] Ggmc, Neslihan; Kauffman, Louis H. On the height of knotoids. Algebraic modeling of topological and computational structures and applications, 259281, Springer Proc. Math. Stat., 219, Springer, Cham, 2017.
- [8] Mikhail Goussarov, Michael Polyak and Oleg Viro, Finite type invariants of classical and virtual knots, math.GT/9810073.

- [9] L. H. Kauffman, *Formal Knot Theory*, Princeton University Press, Lecture Notes Series 30 (1983). Dover Publications (2006).
- [10] L. H. Kauffman, “On Knots”, Princeton University Press (1987).
- [11] Louis H. Kauffman and Heather A. Dye (2005), math.GT/0401035, Minimal surface representations of virtual knots and links. *Algebr. Geom. Topol.* 5 (2005), 509–535.
- [12] Fenn, R.A, Kauffman, L.H, and Manturov, V.O. (2005), Virtual Knots: Unsolved Problems, *Fundamenta Mathematicae*, Proceedings of the Conference “Knots in Poland-2003”, **188**, pp. 293-323.
- [13] Louis H. Kauffman, Detecting virtual knots. *Atti Sem. Mat. Fis. Univ. Modena, Supplemento al Vol. II*, 241-282 (2001).
- [14] Kauffman, L.H. (1987), State Models and the Jones Polynomial, **Topology** **26**, pp. 395-407.
- [15] Kauffman, L.H. (2009), An Extended Bracket Polynomial for Virtual Knots and Links, arXiv:Math:GT/0712.2546, *Journal of Knot Theory and Its Ramifications*, **18**, (6), to appear
- [16] Kauffman, Louis Hirsch. Virtual knot cobordism. in *New ideas in low dimensional topology*, 335377, Ser. Knots Everything, 56, World Sci. Publ., Hackensack, NJ, 2015.
- [17] Kauffman, Louis H. An affine index polynomial invariant of virtual knots. *J. Knot Theory Ramifications* 22 (2013), no. 4, 1340007, 30 pp.
- [18] Manturov, V. O. Parity and cobordisms of free knots. (Russian) *Mat. Sb.* 203 (2012), no. 2, 45–76; translation in *Sb. Math.* 203 (2012), no. 1-2, 196223.
- [19] Ilyutko, D. P.; Manturov, V. O. Cobordisms of free knots. (Russian) *Dokl. Akad. Nauk* 429 (2009), no. 4, 439–441; translation in *Dokl. Math.* 80 (2009), no. 3, 844846.
- [20] Rasmussen, J. A. (2004), Khovanov Homology and the slice genus, ArXivMath:/GT. O402131.
- [21] V.F.R. Jones, A polynomial invariant for links via von Neumann algebras, *Bull. Amer. Math. Soc.* **129** (1985), 103–112.
- [22] V.F.R. Jones. Hecke algebra representations of braid groups and link polynomials. *Ann. of Math.* 126 (1987), pp. 335-338.
- [23] V.F.R. Jones. On knot invariants related to some statistical mechanics models. *Pacific J. Math.*, vol. 137, no. 2 (1989), pp. 311-334.
- [24] L.H. Kauffman, *Knots and Physics*, World Scientific Publishers (1991), Second Edition (1993), Third Edition (2002), Fourth Edition (2012).
- [25] V. O. Manturov, Parity in knot theory’, *Math. sb.* **201**:5, 693–733 (2010) (Original Russian Text in *Mathematical sbornik* **201**:5, pp. 65–110 (2010)).
- [26] Louis H. Kauffman and Heather A. Dye, math.GT/0401035, Minimal surface representations of virtual knots and links. *Algebr. Geom. Topol.* 5 (2005), 509–535.
- [27] H. A. Dye and L. H. Kauffman, Virtual Crossing Number and the Arrow Polynomial. *JKTR*, Vol. 18, No. 10 (October 2009). Page: 1335-1357. arXiv:0810.3858H
- [28] Louis H. Kauffman, Virtual Knot Theory , *European J. Comb.* (1999) Vol. 20, 663-690.
- [29] Louis H. Kauffman, A Survey of Virtual Knot Theory in *Proceedings of Knots in Hellas '98*, World Sci. Pub. 2000 , pp. 143-202.
- [30] Louis H. Kauffman, Detecting Virtual Knots, in *Atti. Sem. Mat. Fis. Univ. Modena Supplemento al Vol. II*, 241-282 (2001).
- [31] Kauffman, Louis H. Introduction to virtual knot theory. *J. Knot Theory Ramifications* 21 (2012), no. 13, 1240007, 37 pp.

- [32] Vassily Olegovich Manturov, Virtual Knot Theory - the state of the art, World Scientific Pub Co. (2012).
- [33] Louis H. Kauffman, math.GT/0405049, A self-linking invariant of virtual knots. *Fund. Math.* 184 (2004), 135–158.
- [34] Louis H. Kauffman, math.GN/0410329, Knot diagrammatics. "Handbook of Knot Theory", edited by Menasco and Thistlethwaite, 233–318, Elsevier B. V., Amsterdam, 2005.
- [35] Greg Kuperberg, What is a virtual link? *arXiv : math.GT/0208039v15Aug2002*
- [36] Kauffman, Louis H. An affine index polynomial invariant of virtual knots. *J. Knot Theory Ramifications* 22 (2013), no. 4, 1340007, 30 pp
- [37] Sang Youl Lee, Towards invariants of surfaces in 4-space via classical link invariants. *Trans. Amer. Math. Soc.*, 361 (2009), 237-265.
- [38] S. Satoh, Virtual knot presentation of ribbon torus-knots, *JKTR*, Vol. 9 No. 4 (2000), pp. 531-542.
- [39] F. Swenton, On a calculus for surfaces and 2-knots in 4-space, *JKTR*, 10 (2001), No. 8, pp. 1133-1141.
- [40] Yasushi Takeda, Introduction to virtual surface-knot theory, *JKTR*, Vol. 21, No. 14, (2012), 1250131 (6 pages).
- [41] Vladimir Turaev, Cobordisms of words. *Commun. Contemp. Math.* 10 (2008), suppl. 1, 927972.
- [42] E. Witten. Quantum Field Theory and the Jones Polynomial. *Comm. in Math. Phys.* Vol. 121 (1989), 351-399.